Supplemental Material

Supplemental Figure 1: INF2 variant localization. (A) Epifluorescence images of transiently transfected GFP-INF2 constructs in HeLa INF2KO cells stably expressing Lifeact-mCherry. Corresponds to Figure 2B. **(B)** Colocalization of GFP-INF2 variants and mCherry-Sec61β as ER marker using epifluorescence. Intensity profiles along dotted lines exemplify degree of overlap. Scale bars: 10 µm.

Supplemental Figure 2: Systematic evaluation of INF2 mutations on actin organization in HeLa wt cells. (A, B) Epifluorescence Images of transiently transfected GFP tagged INF2 constructs (A) in HeLa wt cells stably expressing Lifeact-mCherry (B). **(C)** Quantification of actin intensity ratios of perinuclear over cortical actin in (B), n ≥ 18. INF2 wt and INF2 ΔDID expressing cells were used as positive and negative controls, respectively (black boxes). FSGS and FSGS/CMT linked mutations are labelled in orange and red, respectively. Dashed line indicates average + 2xSD of wt value. Scale bars: 10 µm.

Supplemental Figure 3: Filopodia-like structures induced by INF2 variants. (A, B) TIRFM Images of transiently transfected GFP-INF2 constructs in HeLa INF2 KO cells stably expressing Lifeact-mCherry. Corresponds to Figure 2C. Colocalization in filopodia indicated in (B). **(C)** TIRFM Images of transiently transfected RFP-INF2 constructs in primary podocytes. **(D)** INF2-independent filopodia formed in INF2 wt expressing HeLa cells (above) and primary podocytes (below). Scale bars: 10 µm.

Supplemental Figure 4: Expression analysis of INF2 variants. (A) Western blot showing total protein levels for different INF2 variants transiently expressed in HeLa INF2KO cells. Tubulin levels are shown for comparison. **(B)** Epifluorescence images taken on the Olympus ScanR system showing single cell expression levels of GFP-INF2 variants. **(C, D)** Quantification of transfections efficiencies (C) and GFP intensities in individual cells (D, see methods). Bars indicate Mean ± SEM (N), n > 500 cells, N = 3 experiments. Scale bars: 10 µm.

Supplemental Figure 5: Quantitative analysis of CaAR upon expression of INF2 variants in HeLa wt cells. (A) HeLa wt cells stably expressing Lifeact-mCherry were transfected with indicated GFP-INF2 constructs and followed over time with stimulation for calcium influx by laser ablation at t = 8 s. Images represent GFP-INF2 distribution as well as actin organization at the beginning (t = 0 s) and the time point of maximal actin reorganization (indicated time points in seconds and max(R)). **(B)** Kinetics of actin reorganization observed in (A) given as % change (mean ± SD). **(C)** Box plots max(R) values for analyzed INF2 mutations (n ≥ 21). Wildtype and

ΔDID were used as positive and negative controls (black boxes), respectively. Benign INF2 variants, FSGS and FSGS/CMT linked mutations are labelled in green, orange and red, respectively. Values are ordered first by type of INF2 mutation and then by difference to ΔDID value (largest to smallest). Scale bar: 10 µm.

Supplemental Figure 6: Quantitative analysis of CaAR upon expression of INF2 variants in AB8 INF2KO podocytes. (A) AB8 INF2KO cells were transiently transfected with Lifeact-mCherry and indicated GFP-INF2 constructs and followed over time with stimulation for calcium influx by laser ablation at t = 8 s. Images represent GFP-INF2 distribution as well as actin organization at the beginning (t = 0 s) and the time point of maximal actin reorganization (indicated time points in seconds and max(R)). **(B)** Kinetics of actin reorganization observed in (A) given as % change (mean ± SD). **(C)** Scatter plots of max(R) values for analyzed INF2 mutations (n ≥ 8). Wildtype and ΔDID were used as positive and negative controls (black dots), respectively. FSGS and FSGS/CMT linked mutations are labelled in orange and red, respectively. Scale bar: 10 µm.

Supplemental Figure 7: Sns distribution in fly nephrocytes. Fly nephrocytes stably expressing the indicated Myc-INF2 mutants were heat fixed and analyzed for nephrin (Sns) localization using anti-Sns antibody. Images represent medial planes of shown nephrocytes with zoomed areas to illustrate density of Sns in the plasma membrane. See Figure 6 for surface sections. Scale bars: 10 µm.

Video 1. CaAR in primary podocytes. Primary podocyte transiently expressing Lifeact-mCherry. Cell was stimulated with 500 nM ionomycin at t = 0 s. Corresponds to Figure 1A. Scale bar: 10 µm.

Video 2. INF2 variants in primary podocytes. Z-series of primary podocytes transiently expressing RFP-INF2 variants. Planes were acquired at 100 nm steps. Corresponds to Figure 1B. Scale bar: 10 µm.

Video 3. Filopodia formation by INF2 variants. TIRFM series of HeLa INF2 KO cells transiently expressing indicated GFP-INF2 variants. Corresponds to Figure 2C. Scale bar: 10 µm.

Video 4. CaAR with INF2 variants. Epifluorescence series of HeLa INF2 KO cells stably expressing Lifeact-mCherry and transiently expressing indicated GFP-INF2 variants. Cells were stimulated by laser ablation at t = 8 s. Corresponds to Figure 3A. max(R) indicates thresholded image. Time in min:s. Scale bar: 10 µm.

Video 5. Actin association of INF2 DID. TIRFM series of HeLa INF2 KO cells transiently expressing GFP-INF2 DID domain. Cells were stimulated by laser ablation at t = 8 s. Associated to Figure 5A. Time in min:s. Scale bar: 10 µm.

Video 6. Actin association of INF2 DID variants. TIRFM series of HeLa INF2 KO cells transiently expressing indicated GFP-INF2 DID domain variants and Lifeact-mCherry. Cells were stimulated by laser ablation at t = 8 s. Associated to Figure 5. Scale bar: 10 µm.

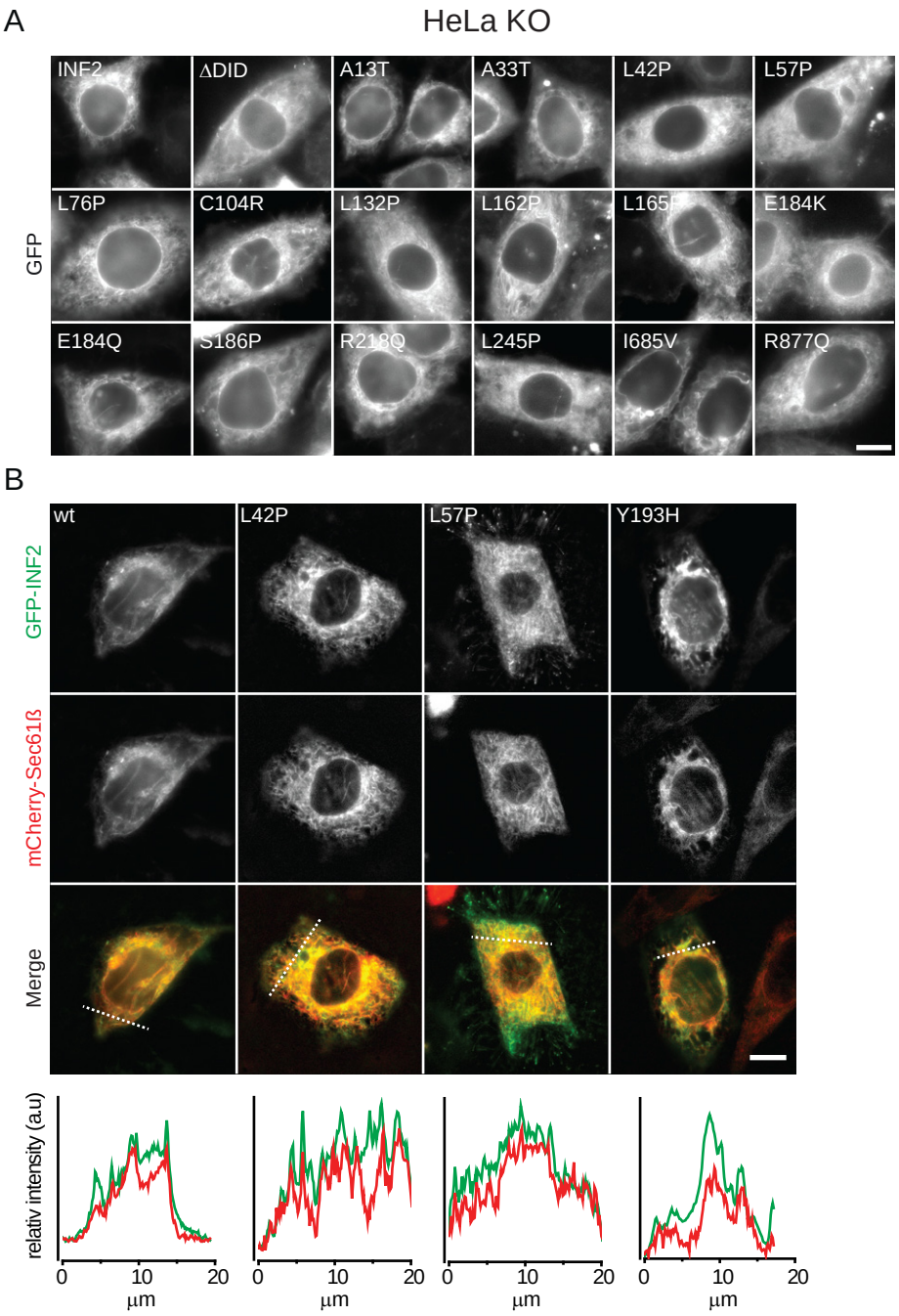
A
HeLa KO
GFP
INF2
ΔDID
A13T
A33T
L42P
L57P
L76P
C104R
L132P
L162P
L165
E184K
E184Q
S186P
R218Q
L245P
I685V
R877Q
B
wt
L42P
L57P
Y193H
GFP-INF2
mCherry-Sec61ß
Merge
relativ intensity (a.u)
0
10
20
µm

Figure S1

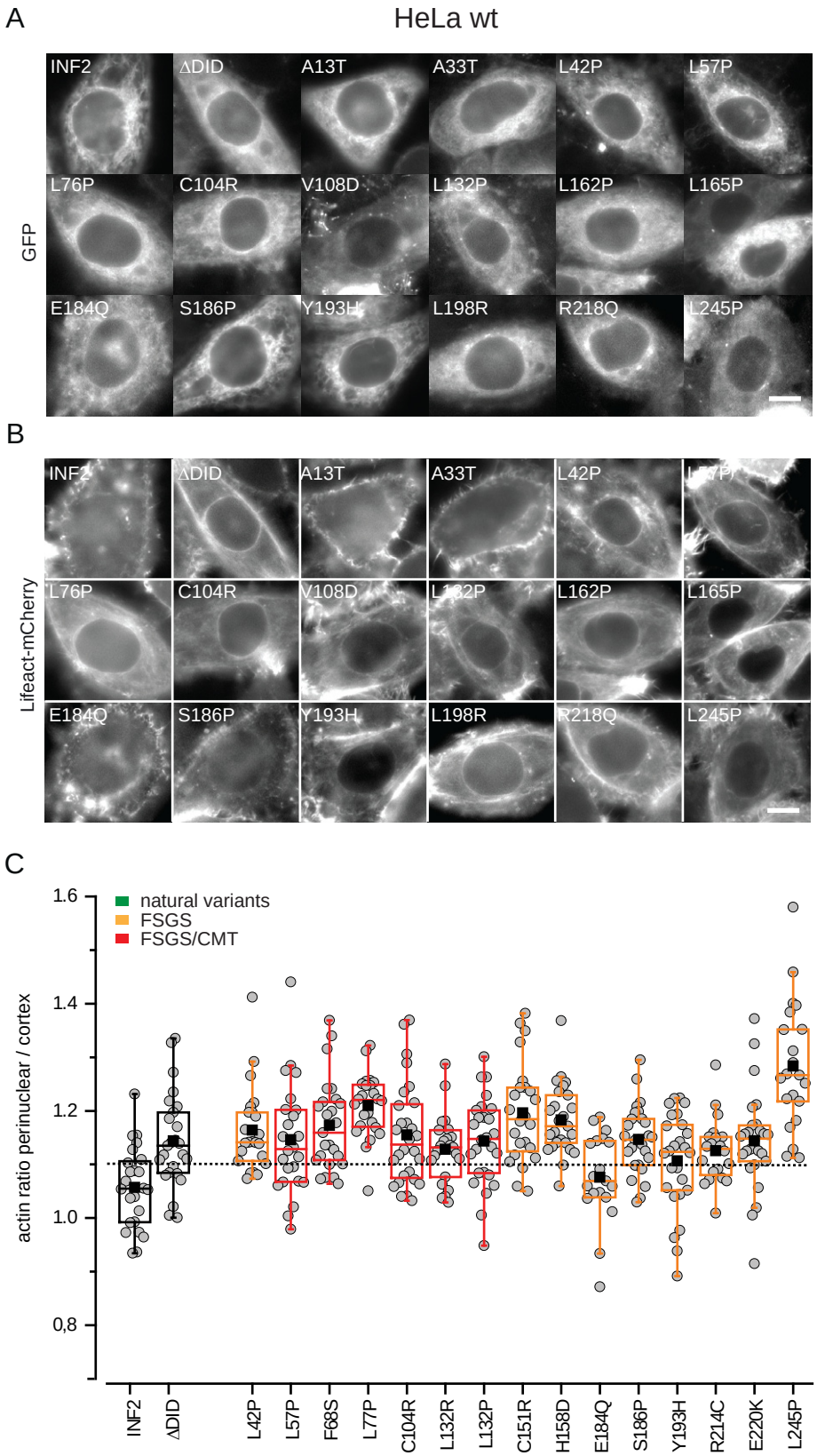
A
HeLa wt
GFP
INF2
ΔDID
A13T
A33T
L42P
L57P
L76P
C104R
V108D
L132P
L162P
L165P
E184Q
S186P
Y193H
L198R
R218Q
L245P
B
Lifeact-mCherry
C
natural variants
FSGS
FSGS/CMT
actin ratio perinuclear / cortex
1.6
1.4
1.2
1.0
0,8
INF2
ΔDID
L42P
L57P
F68S
L77P
C104R
L132R
L132P
C151R
H158D
E184Q
S186P
Y193H
R214C
E220K
L245P

Figure S2

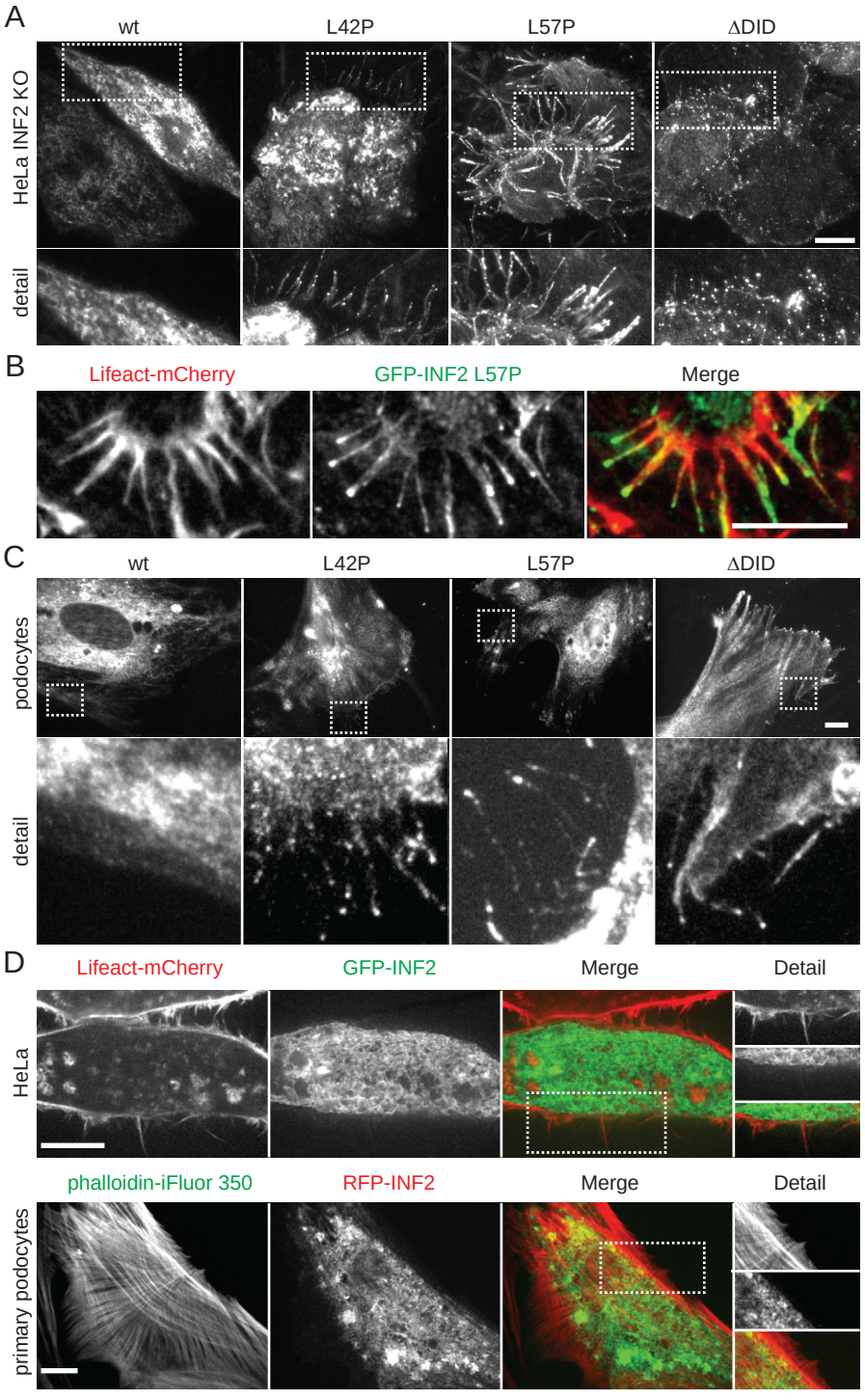
A
wt
L42P
L57P
ΔDID
HeLa INF2 KO
detail
B
Lifeact-mCherry
GFP-INF2 L57P
Merge
C
wt
L42P
L57P
ΔDID
podocytes
detail
D
Lifeact-mCherry
GFP-INF2
Merge
Detail
HeLa
phalloidin-iFluor 350
RFP-INF2
Merge
Detail
primary podocytes

Figure S3

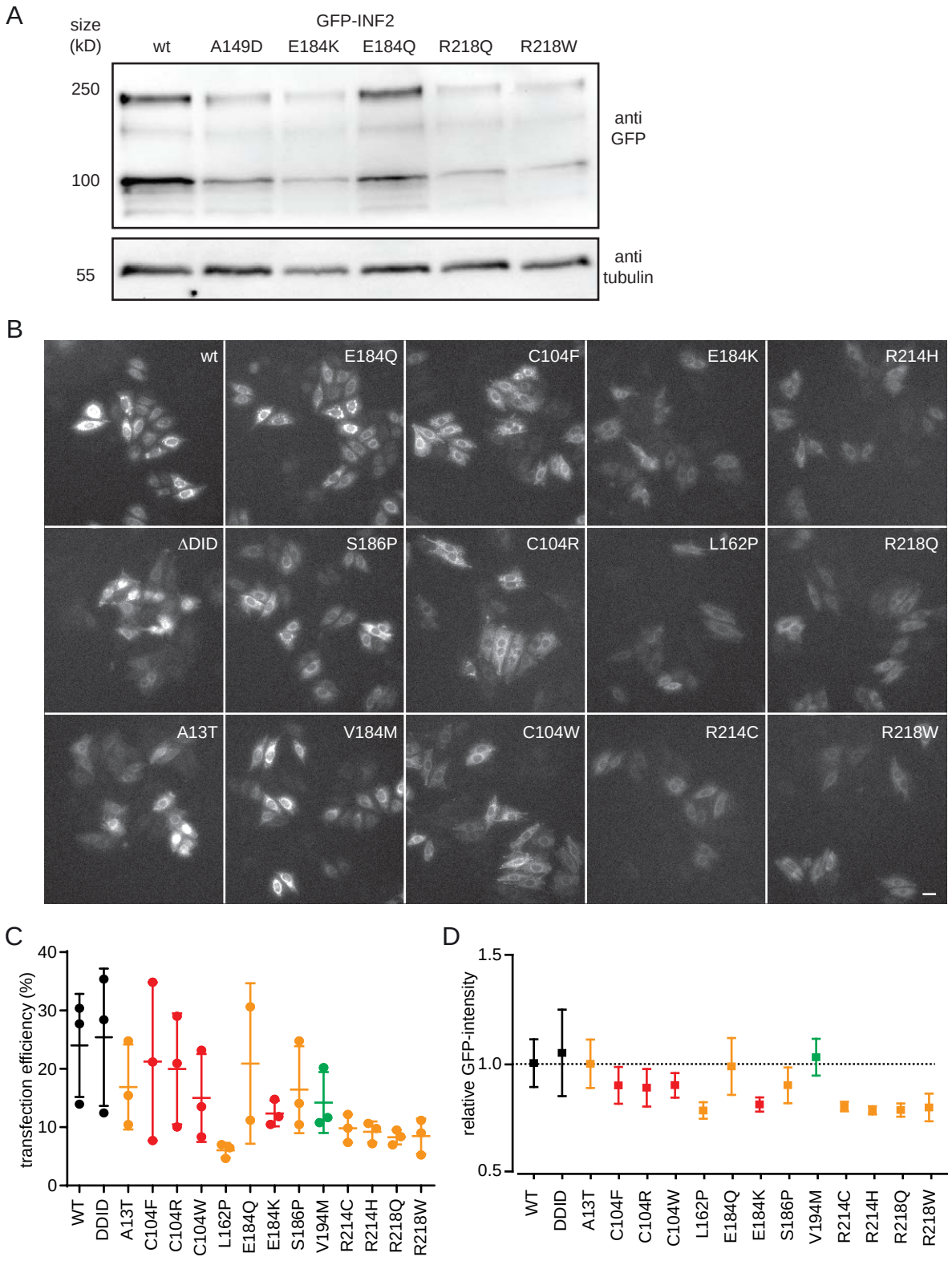
A
size
(kD)
GFP-INF2
wt
A149D
E184K
E184Q
R218Q
R218W
250
100
55
anti
GFP
anti
tubulin
B
wt
E184Q
C104F
E184K
R214H
ΔDID
S186P
C104R
L162P
R218Q
A13T
V184M
C104W
R214C
R218W
C
transfection efficiency (%)
40
30
20
10
0
WT
DDID
A13T
C104F
C104R
C104W
L162P
E184Q
E184K
S186P
V194M
R214C
R214H
R218Q
R218W
D
relative GFP-intensity
1.5
1.0
0.5
WT
DDID
A13T
C104F
C104R
C104W
L162P
E184Q
E184K
S186P
V194M
R214C
R214H
R218Q
R218W

Figure S4

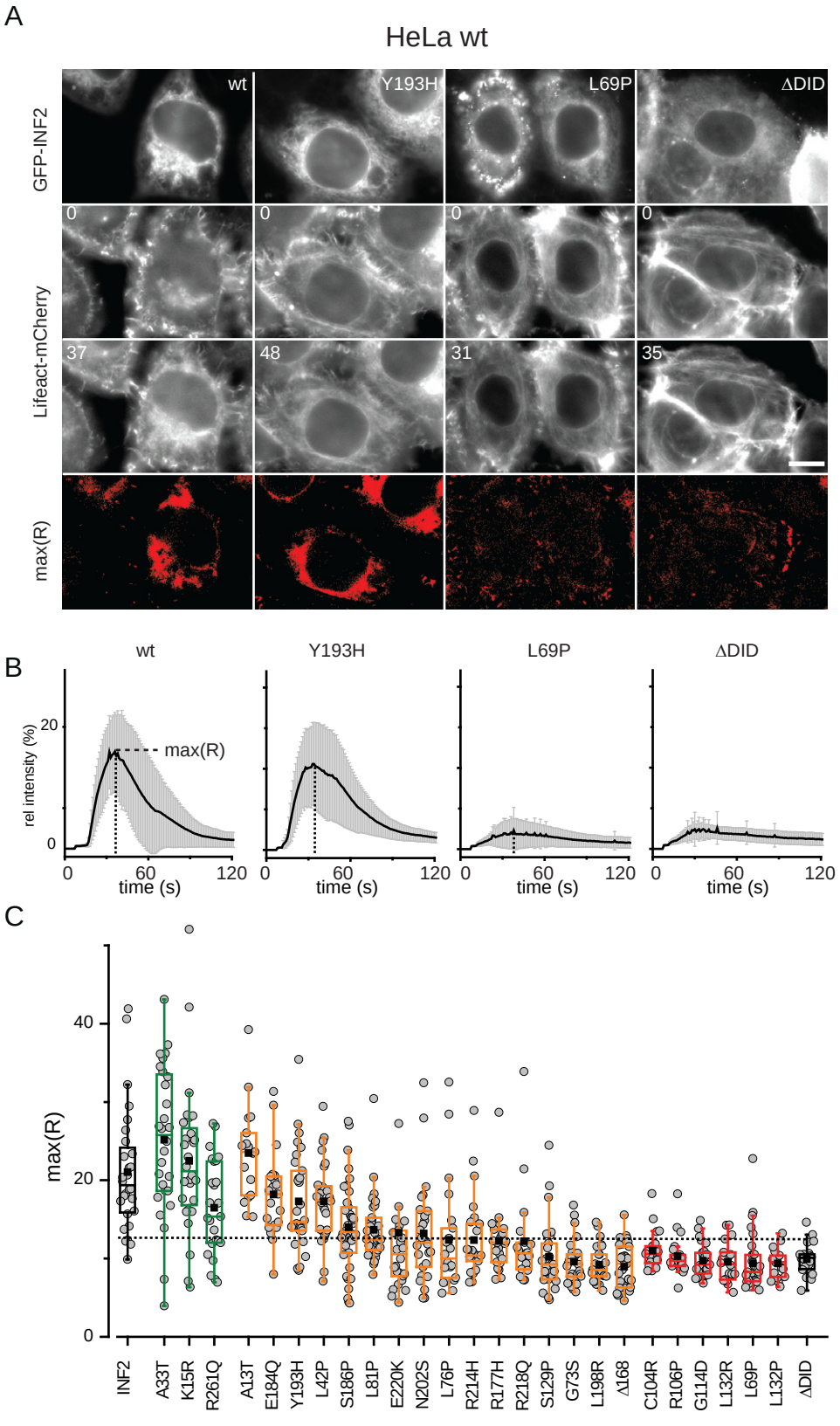
A
HeLa wt
wt
Y193H
L69P
ΔDID
GFP-INF2
Lifeact-mCherry
max(R)
0
37
48
31
35
B
rel intensity (%)
max(R)
time (s)
C
max(R)
INF2
A33T
K15R
R261Q
A13T
E184Q
Y193H
L42P
S186P
L81P
E220K
N202S
L76P
R214H
R177H
R218Q
S129P
G73S
L198R
Δ168
C104R
R106P
G114D
L132R
L69P
L132P
ΔDID

Figure S5

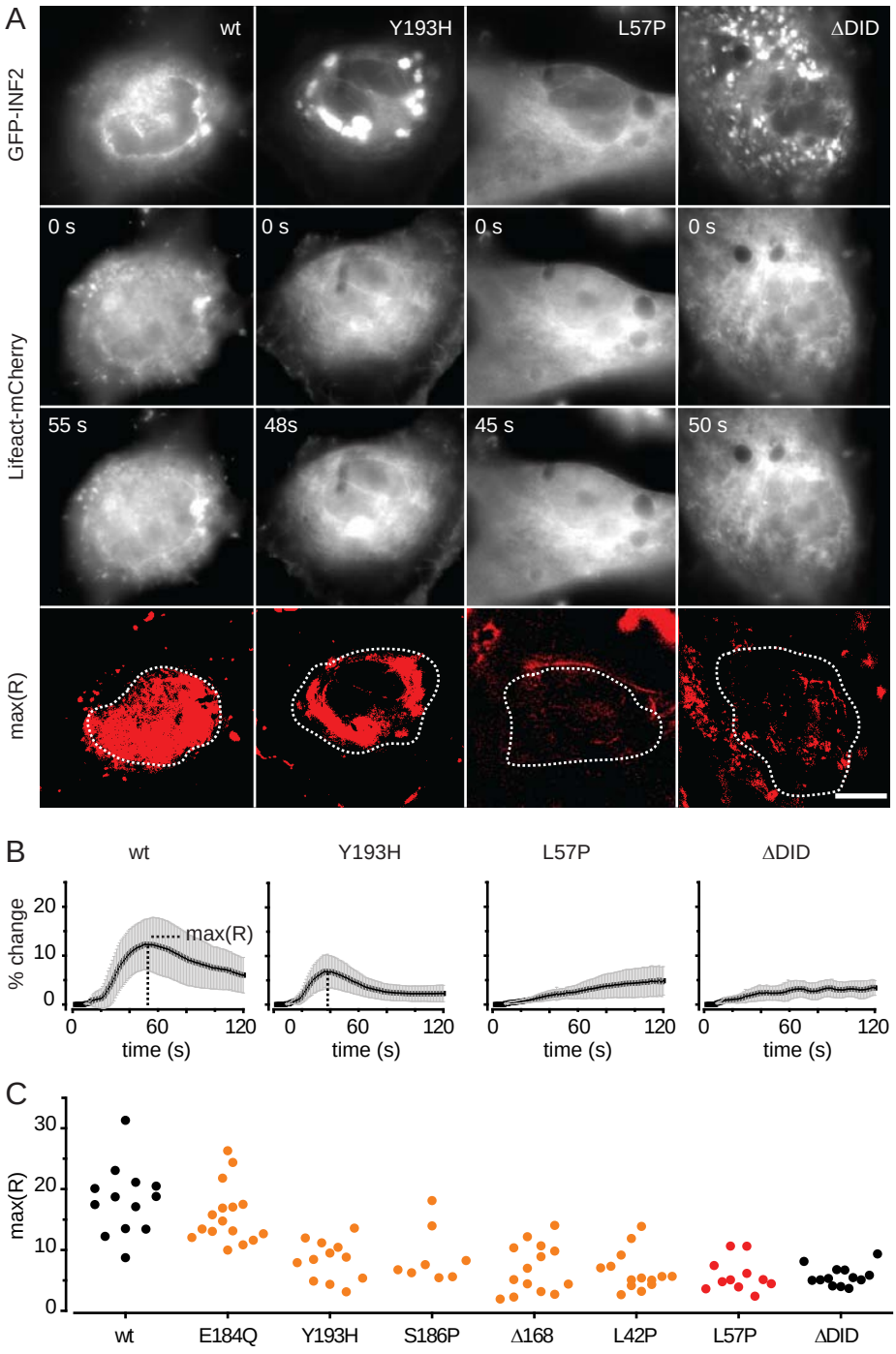
A
wt
Y193H
L57P
ΔDID
GFP-INF2
Lifeact-mCherry
0 s
0 s
0 s
0 s
55 s
48s
45 s
50 s
max(R)
B
wt
Y193H
L57P
ΔDID
% change
20
10
0
max(R)
0
60
120
time (s)
C
max(R)
30
20
10
0
wt
E184Q
Y193H
S186P
Δ168
L42P
L57P
ΔDID

Figure S6

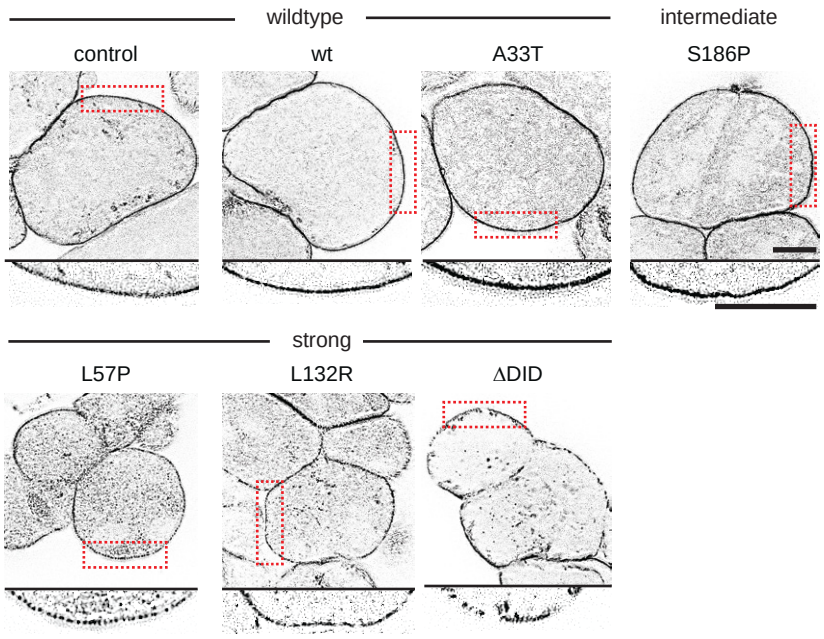
wildtype
intermediate
control
wt
A33T
S186P
strong
L57P
L132R
ΔDID

Figure S7